

Integrated human organ-on-a-chip models for predictive studies of anti-tumor drug efficacy and cardiac safety

Alan Chramiec,* Diogo Teles,* Keith Yeager, Alessandro Marturano-Kruik, Joseph Pak, Timothy Chen, Luke Hao, Miranda Wang, Roberta Lock, Daniel Naveed Tavakol, Marcus Busub Lee, Jinho Kim, Kacey Ronaldson-Bouchard, and Gordana Vunjak-Novakovic#

Columbia University, 622 West 168th Street, VC 12-234, New York NY, 10032, USA. +1 (212) 305-2304, gv2131@columbia.edu

* Authors contributed equally.

Supplemental material

VIDEOS

Supplemental Video 1. Assembly of the platform.

Supplemental Video 2. Media velocity in the platform.

Supplemental Video 3. Representative video of cardiac tissue before linsitinib treatment in isolation.

Supplemental Video 4. Representative video of cardiac tissue after linsitinib treatment in isolation.

Supplemental Video 5. Representative video of cardiac tissue before linsitinib treatment in the integrated platform.

Supplemental Video 6. Representative video of cardiac tissue after linsitinib treatment in the integrated platform.

TABLES

Supplemental Table 1. Dimensions and other parameters of the platform.

FIGURES

Supplemental Figure 1. Study design.

Supplemental Figure 2. Integrated heart-bone platform.

Supplemental Figure 3. Multi-organ platform modularity.

Supplemental Figure 4. In-house built microscope system for visualizations of the tissues cultured in the platform.

Supplemental Figure 5. Immunohistochemical (IHC) staining of engineered ES tumors with transduced GFP-luciferase positive cancer cells.

Supplemental Figure 6. Evaluation of the dose-dependent effects of linsitinib concentration on metastatic and non-metastatic Ewing sarcoma cell line monolayers.

Supplemental Figure 7. Evaluation of the dose-dependent effects of doxorubicin and linsitinib on engineered non-metastatic and metastatic ES bone tumors.

Supplemental Figure 8. Determining the effects of linsitinib on ES cells and osteoblasts within the engineered ES bone tumors across a 3-week clinical drug treatment regimen.

Supplemental Figure 9. Calcium handling of cardiac tissues exposed to linsitinib in isolation.

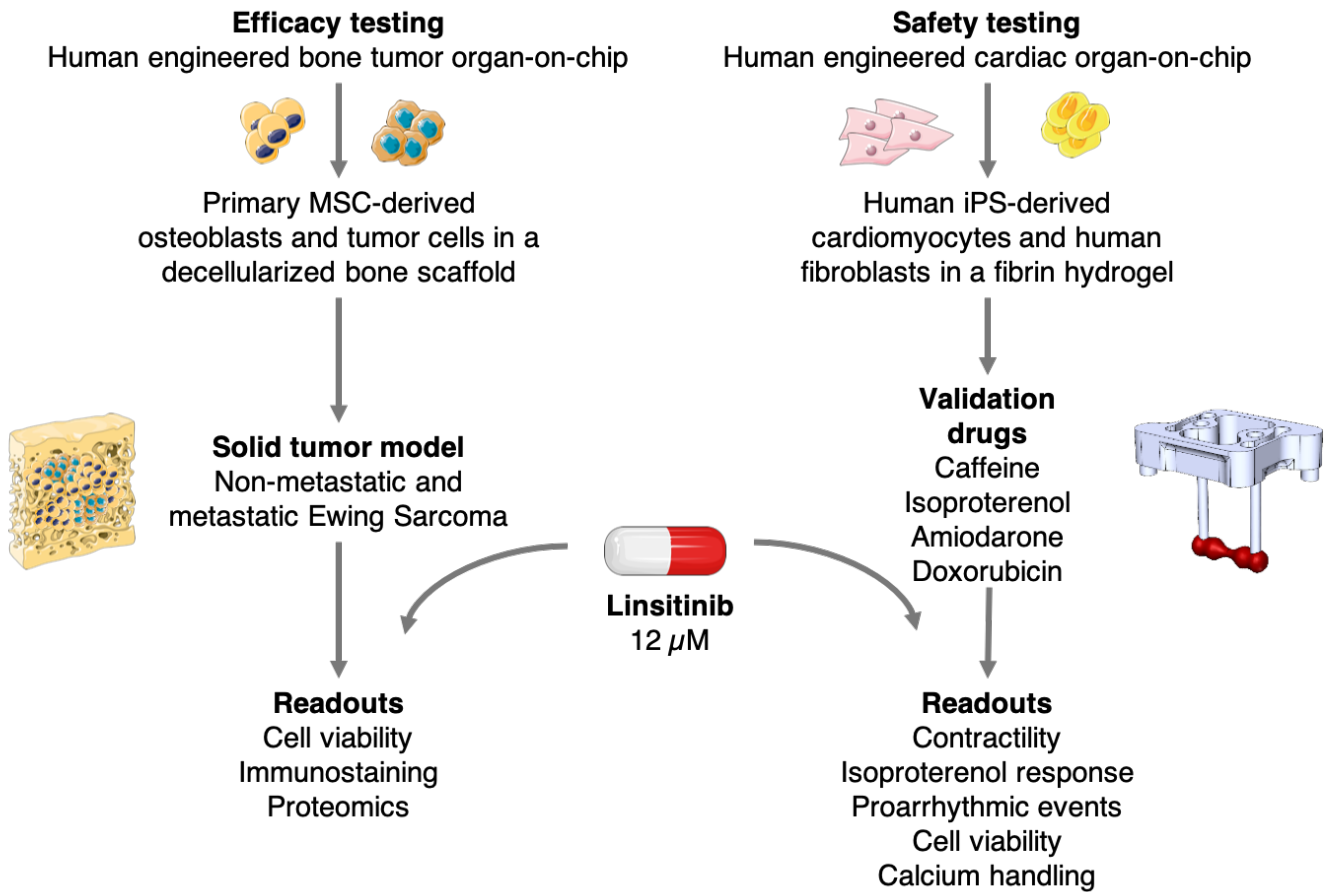
Supplemental Figure 10. Assessment of the effects of integrated platform culture media conditions on engineered bone tumor and cardiac tissues.

Supplemental Figure 11. Evaluation of IGFBP-3 expression and effects on survivability across ES patient populations and the role of drug diffusion in the response of non-metastatic engineered ES bone tumor to linsitinib in the integrated platform.

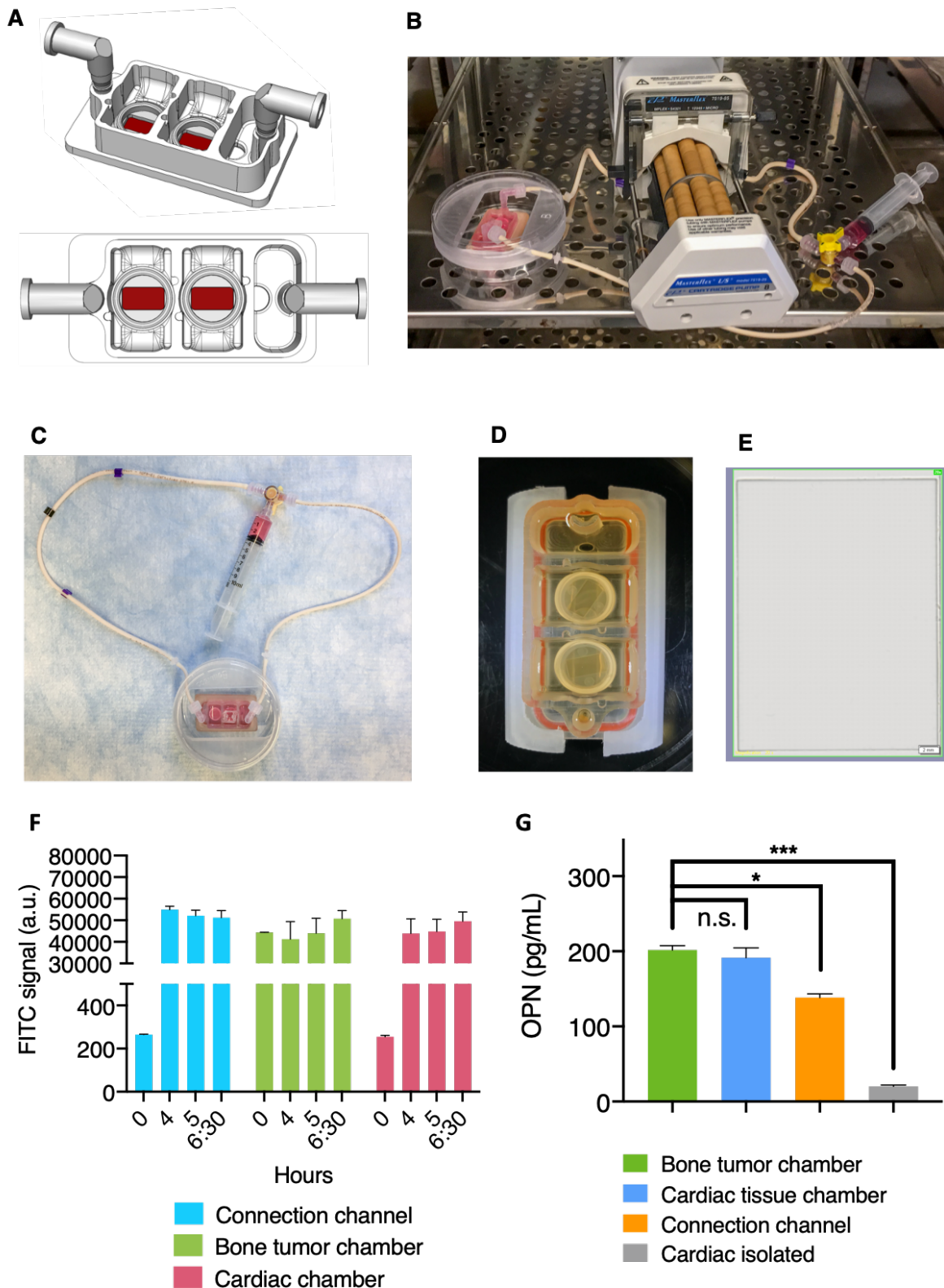
Supplemental Figure 12. Calcium handling of cardiac tissues after exposure to linsitinib in the integrated platform.

| | |
|----------------------------------|-----------------------|
| Length | 60 mm |
| Height | 20 mm |
| Width | 26 mm |
| Height of the connection channel | 0.3 mm |
| Length of the connection channel | 5 mm |
| Overall diameter of transwell | 12 mm |
| Porous mesh area of transwell | 8 x 4 mm |
| Transwell pores | 20 μm |
| Circulating volume | 5 mL |
| Chamber volume | 1.5 mL |
| Flow rate | 3.3 mL/min |
| Shear stress | 5 dyn/cm ² |

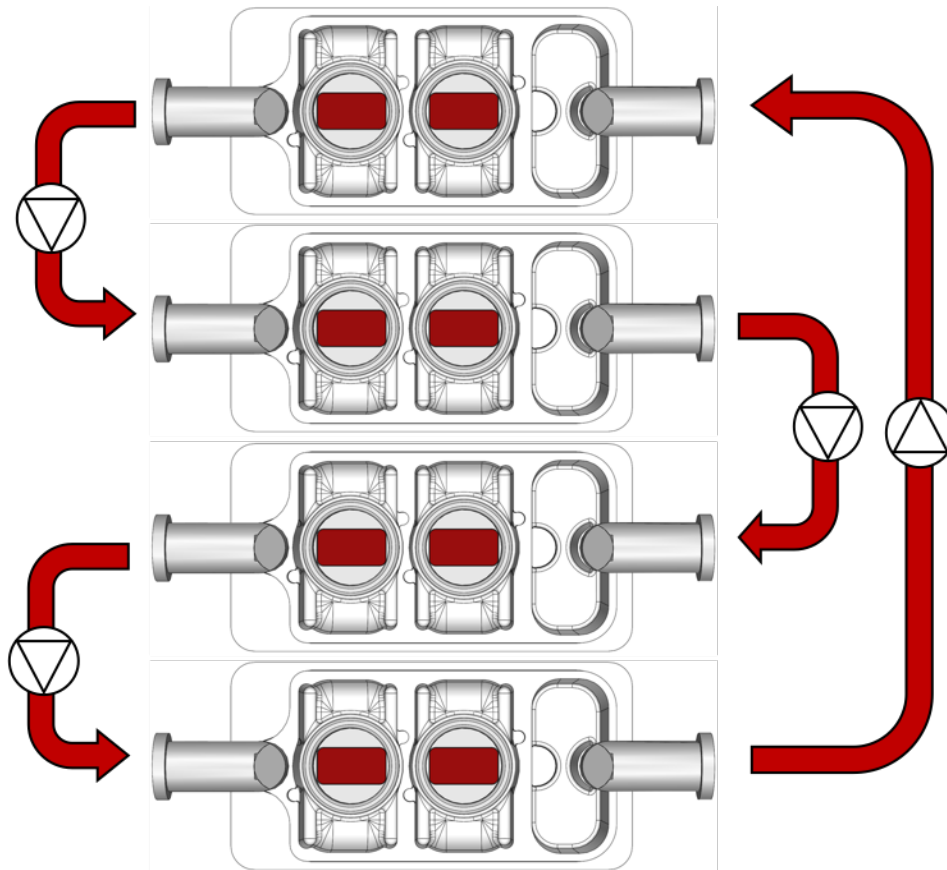
Supplemental Table 1. Dimensions and other parameters of the platform.



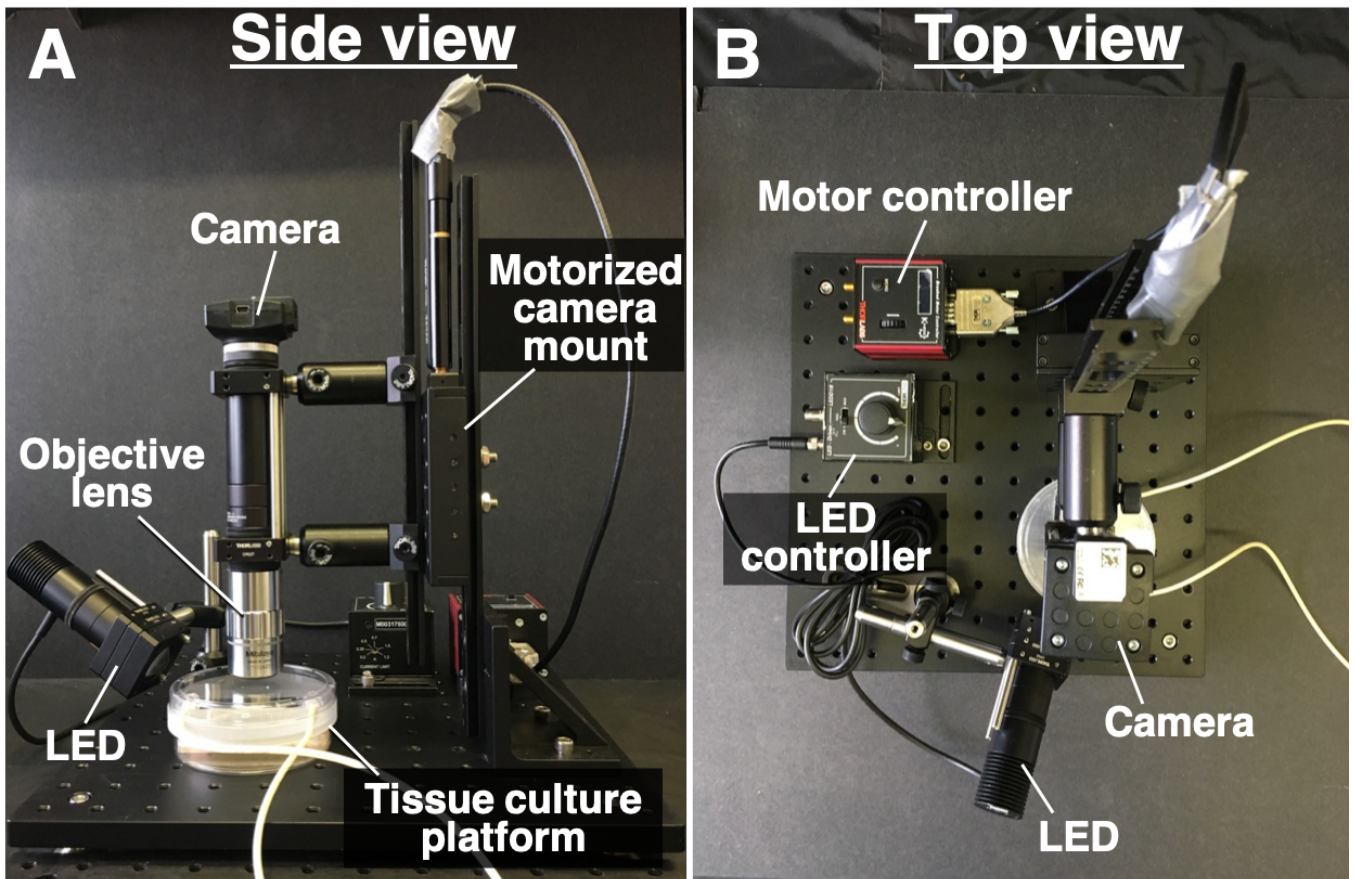
Supplemental Figure 1. Study design. We developed two different organs-on-chips to evaluate anti-cancer drug efficacy (using a bioengineered human Ewing sarcoma tumor) and cardiac safety (using a bioengineered human cardiac tissue). Both organs were generated with human cells and characterized and validated before being exposed to linsitinib, a novel anti-cancer therapeutic agent, in isolated culture and within the novel platform with microfluidic perfusion.



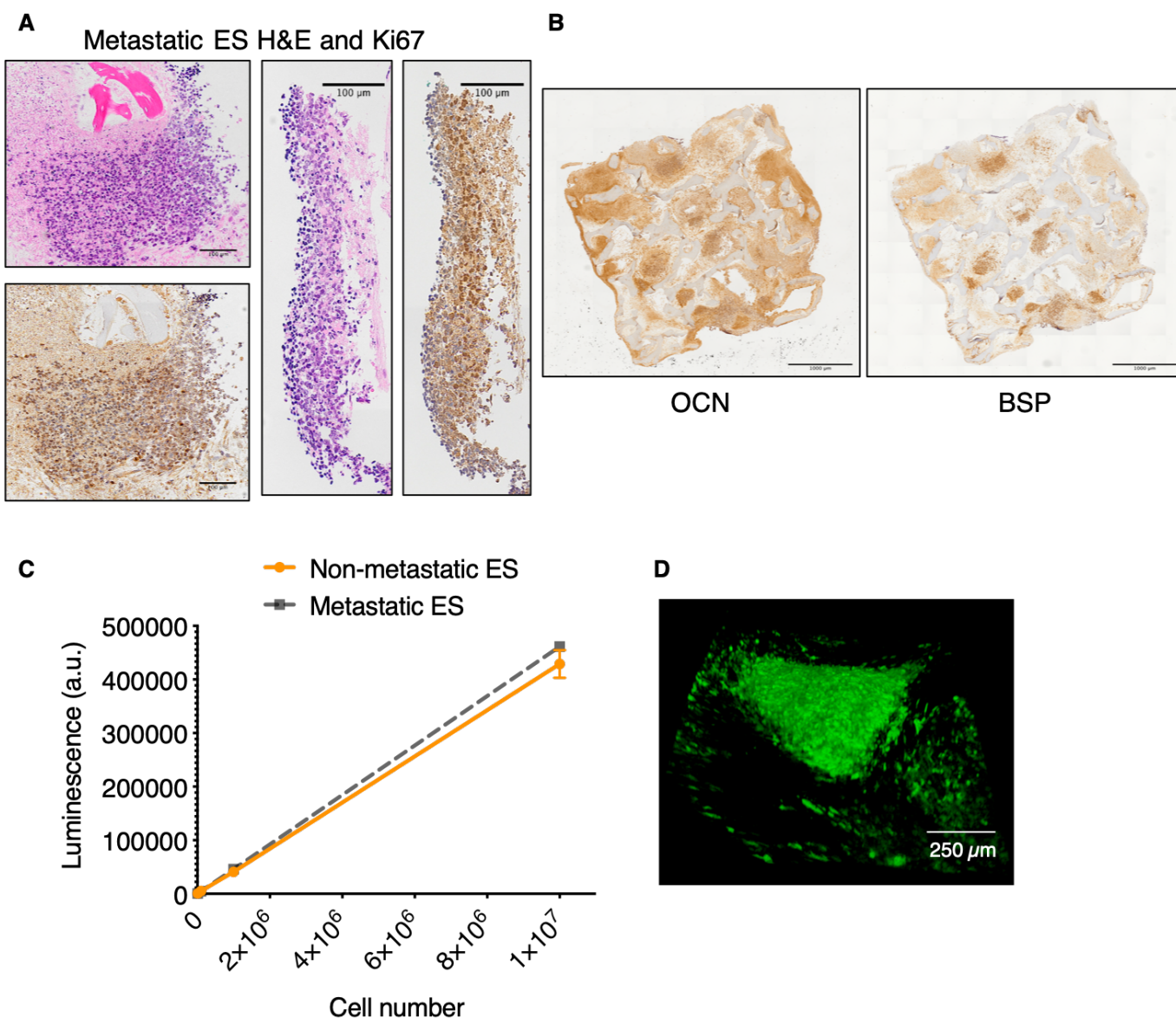
Supplemental Figure 2. Integrated heart-bone tumor platform. **A.** Photo of the assembled platform. **B.** Platform connected to a peristaltic pump in an incubator. **C.** Bacterial and fungal culture media remained clear after 4 weeks of culture in the platform. **D&E.** Under the naked eye (**D**) and microscopic observation (**E**), no presence of microorganisms in the bacteria and fungi specific media after 4 weeks of culture in the platform. Scale = 2 mm. **F.** Empirical FITC concentrations in all chambers of the platform, after being added in the bone tumor chamber. FITC was assessed at 0, 4, 5, and 6:30 hours (mean \pm s.e.m., $n = 3$). **G.** Osteopontin concentration (pg/mL) was assessed in supernatants collected from all chambers of the platform after a 3-days integrated culture, as well from an isolated cardiac tissue (mean \pm s.e.m., $n = 4$). * $P < 0.05$; ** $P < 0.01$; *** $P < 0.001$; by two-way ANOVA with Bonferroni post-test.



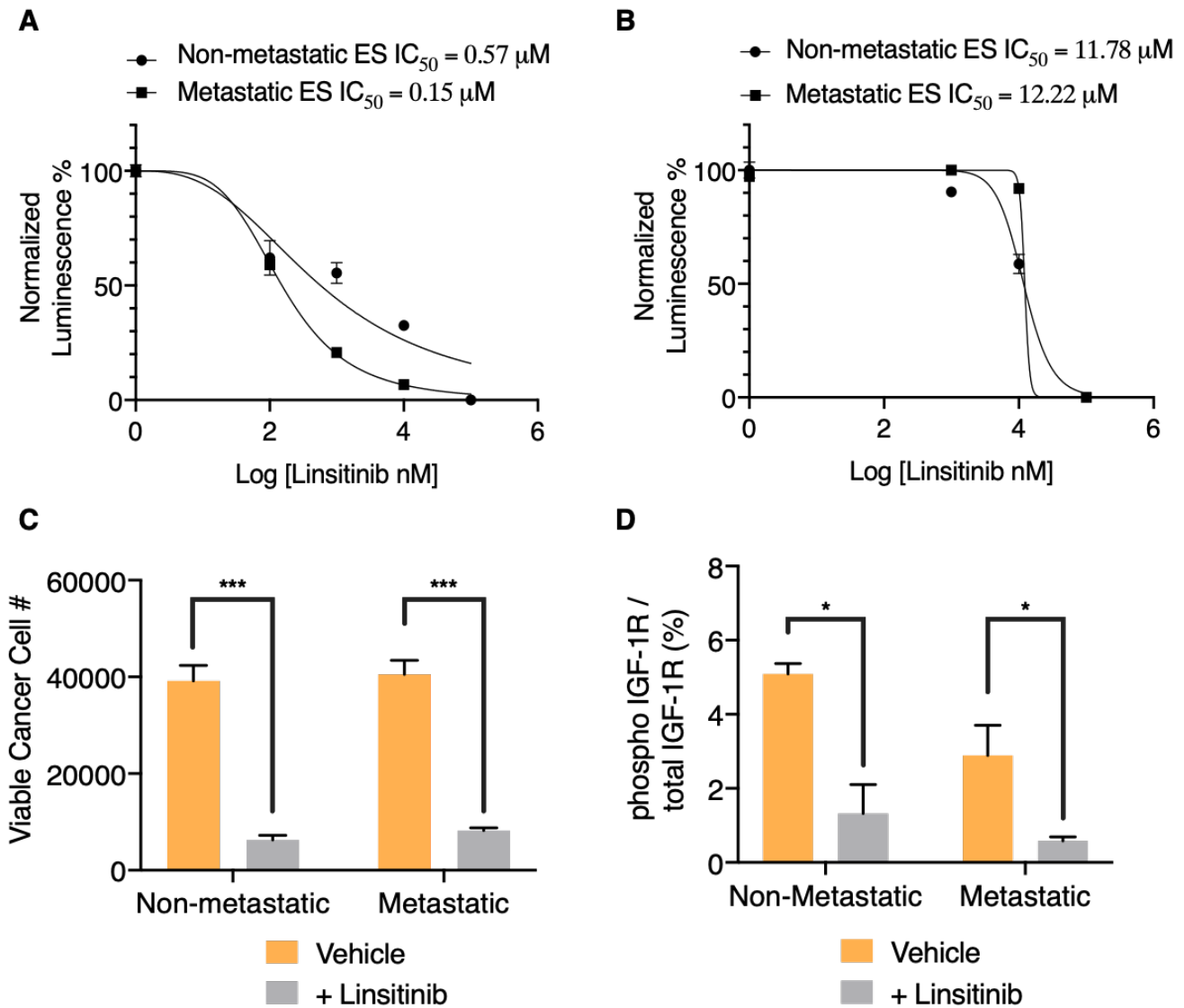
Supplemental Figure 3. Multi-organ platform modularity. Complexity of the platform is user-determined, from a single to multiple serial connected platforms (in this example, 8 tissues serial connection), for scaling of the system.



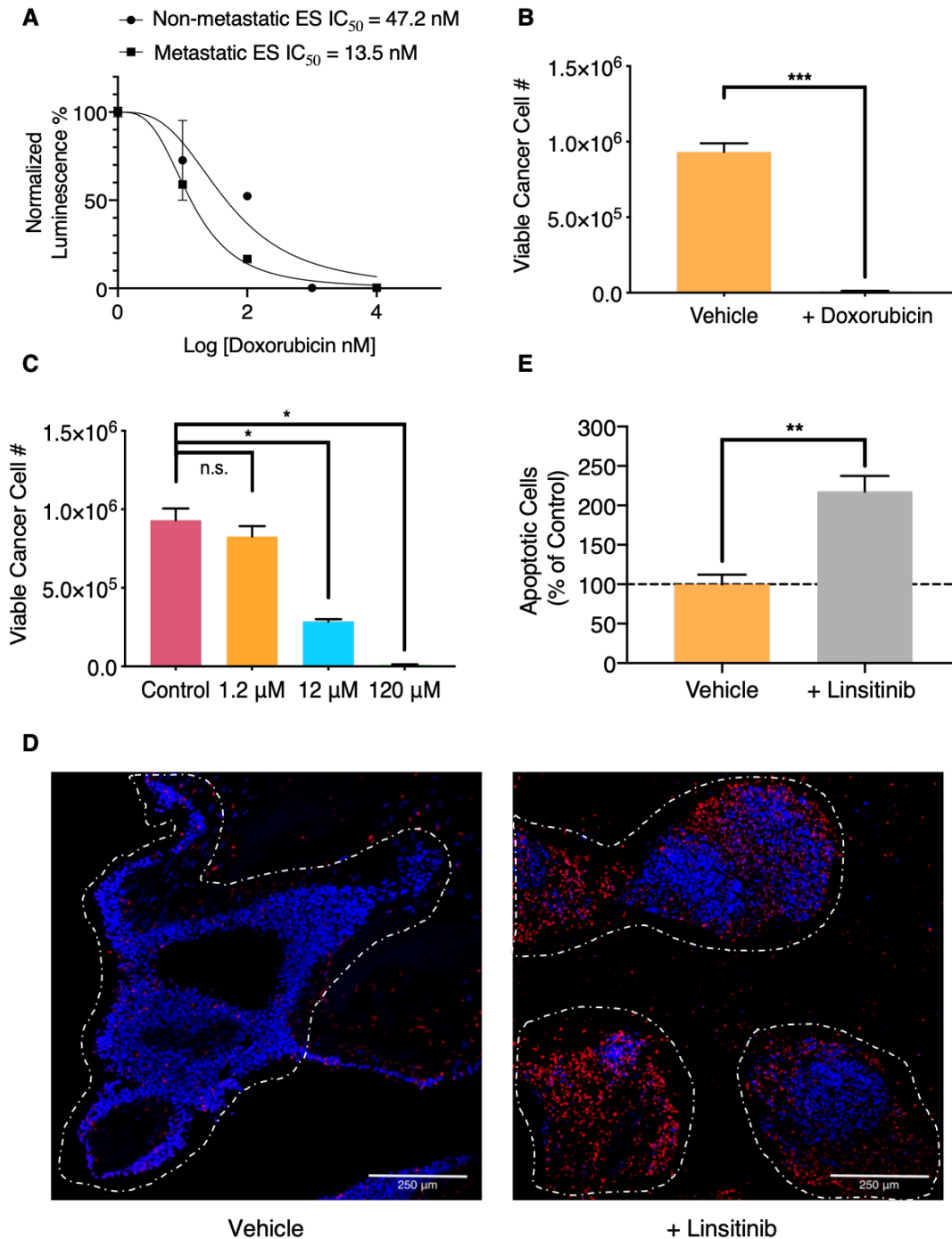
Supplemental Figure 4. In-house built microscope system for visualization of the tissues cultured in the platform. A & B. Side (A) and top (B) view of the microscope system constructed using commercially available optomechanical components. To image the tissues in the platform, we incorporated a 2X microscopic objective lens (Mitutoyo Inc.) with a long working distance (34 mm) into the imaging system. The exchangeable LED light source allows both bright-field and fluorescent imaging. The motorized camera mount enables precise focus of different imaging planes across the tissue surfaces.



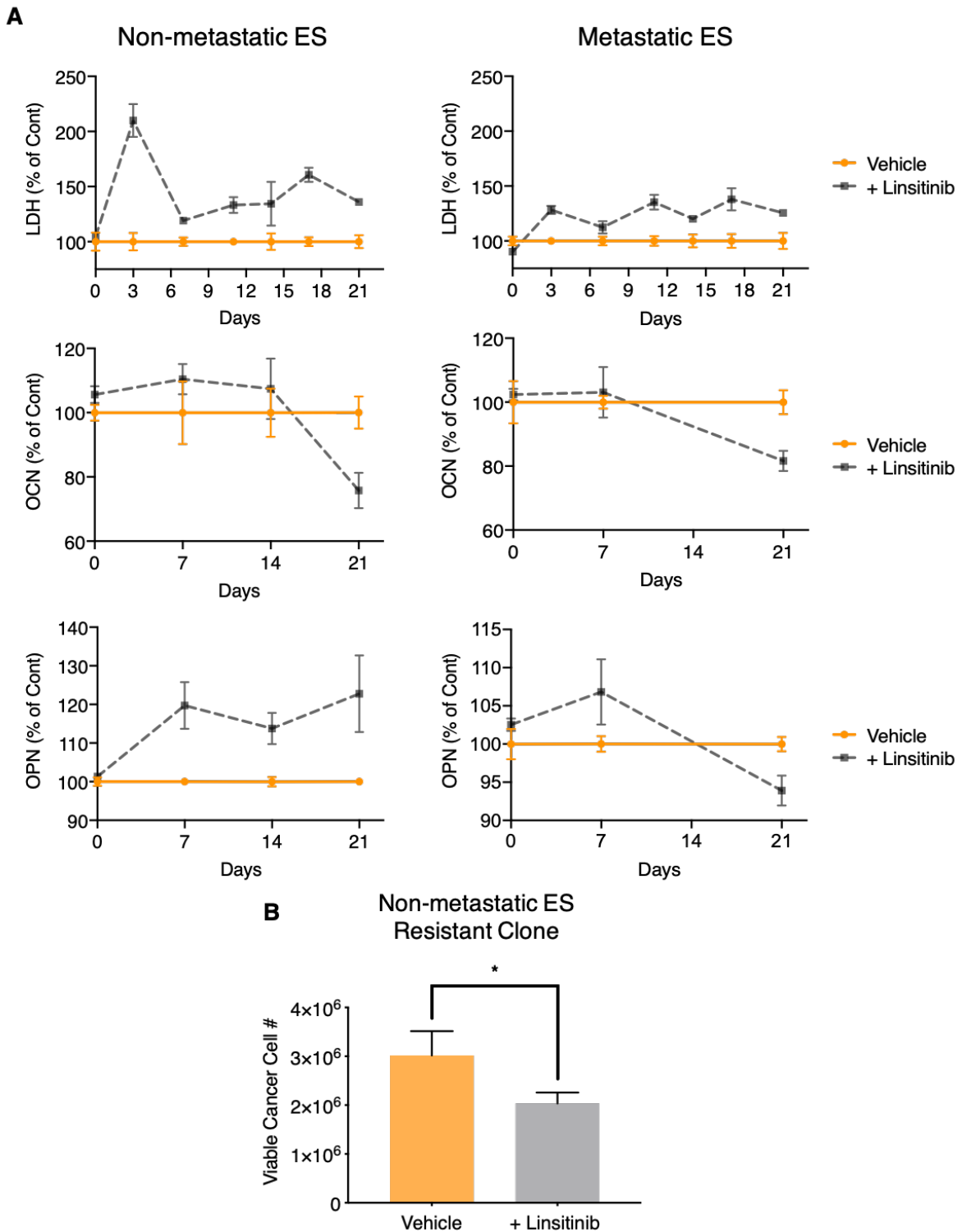
Supplemental Figure 5. Immunohistochemical (IHC) staining of engineered ES tumors with transduced GFP-luciferase positive cancer cells. **A.** H&E staining and parallel IHC analysis of proliferation marker Ki67 of the metastatic ES engineered tissue. Variability in tumor morphology and the numbers of proliferative Ki67 positive cancer cells demonstrates ability to recreate some degree of intra- and inter-tumor heterogeneity. **B.** IHC staining of engineered bone tumors showing positivity for mature, functional osteoblast markers osteocalcin (OCN) and sialoprotein (BSP). **C.** Monolayers of each of the transduced and sorted GFP-luciferase positive ES cancer cell lines (non-metastatic and metastatic) were formed (using 10^4 , 10^5 , and 10^6 cells per well) and the luminescence signal was measured (mean \pm s.e.m., $n = 3$) to determine if it could serve as an effective function of cell number and viability. **D.** Confocal microscopy image of an GFP-luciferase positive engineered bone tumor in situ on the engineered human bone tissue, mineral bone scaffold. All scale bars: 100 or 250 μm , as noted.



Supplemental Figure 6. Evaluation of the dose-dependent effects of linsitinib concentration on metastatic and non-metastatic Ewing sarcoma cell line monolayers. **A.** Non-metastatic and metastatic ES cell lines were treated with various concentrations of linsitinib (0, 0.1, 1, 10, and 100 μM) over 72 hours. MTT viability assay was used to determine drug toxicity, with luminescence generated by viable cells measured at the endpoint (10^4 cells per well, mean \pm s.e.m., $n = 3$). **B.** Non-metastatic and metastatic GFP-luciferase transduced, positive ES cell lines were treated with various concentrations of linsitinib (0, 0.1, 1, 10, and 100 μM) over 72 hours. In order to determine cancer cell viability, cells were lysed and treated with luciferin using a Bright-GloTM assay, with subsequent luminescence measured (10^4 cells per well, mean \pm s.e.m., $n = 3$). **C.** Non-metastatic and metastatic GFP-luciferase transduced, positive ES cell monolayers were treated with 12 μM linsitinib for 72 hours and viability was determined by measuring luminescence of these cells (10^4 cells per well, mean \pm s.e.m., $n = 3$). **D.** Non-metastatic and metastatic ES cell lines were treated with 12 μM linsitinib for 6 hours, lysed, measured for protein quantity using a standard BCA protein quantification assay, and loaded equally onto an ELISA to semi-quantitatively determine phosphorylated levels of the IGF-1 receptor vs total IGF-1 receptor (mean \pm s.e.m., $n = 4$). * $P < 0.05$; ** $P < 0.01$; *** $P < 0.001$ by unpaired two-tailed Student's t test.



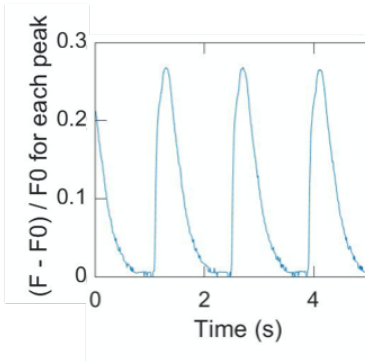
Supplemental Figure 7. Evaluation of the dose-dependent effects of doxorubicin and linsitinib on engineered non-metastatic and metastatic ES bone tumors. **A.** Non-metastatic and metastatic ES cell lines were treated with various concentrations of doxorubicin (0, 10, 100, 1,000, and 10,000 nM) over 72 hours. An MTT viability assay was used to determine drug toxicity, with luminescence generated by viable cells measured at the endpoint (10^4 cells per well, mean \pm s.e.m., $n = 3$). **B.** Non-metastatic engineered ES bone tumors were treated with 1 μ M doxorubicin for 72 hours and viability was determined by measuring luminescence of these cells (mean \pm s.e.m., $n = 3$). **C.** Non-metastatic engineered ES bone tumors were treated using a range of concentrations of linsitinib (0, 1.2, 12, and 120 μ M) for 72 hours and viability was determined by measuring luminescence of these cells (mean \pm s.e.m., $n = 3$). **D.** TUNEL analysis for apoptosis of untreated (*left*) and 12 μ M linsitinib treated (*right*) non-metastatic engineered ES bone tumors. Tumors are outlined by white dashes and validated using corresponding H&E stains of the identical loci. All scale bars: 250 μ m. **E.** TUNEL Cell Counter software was used to analyze the TUNEL stain images to determine absolute numbers of apoptotic cells per representative image (mean \pm s.e.m., $n = 4$). * $P < 0.05$; ** $P < 0.01$; *** $P < 0.001$ by two-way ANOVA with Bonferroni post-test or unpaired two-tailed Student's *t* test.



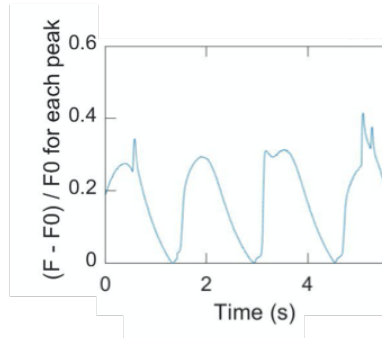
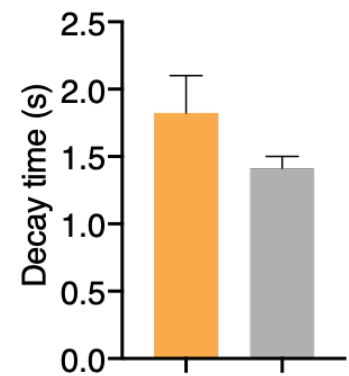
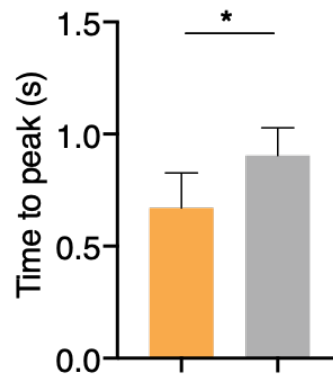
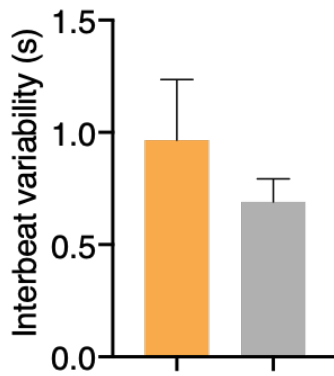
Supplemental Figure 8. Determining the effects of linsitinib on ES cells and osteoblasts within the engineered ES bone tumors across a 3-week clinical drug treatment regimen. A. Non-metastatic (left) and metastatic (right) engineered ES bone tumors were exposed to linsitinib (12 μ M) according to the 3-week drug treatment regimen used in a clinical study we aimed to recapitulate. Supernatants were collected from each individual sample across the duration of the drug treatments and were analyzed for osteoblast function (OCN, OPN) and for cytotoxicity (LDH) (mean \pm s.e.m., n = 3). **B.** Linsitinib resistant cancer cells from the responsive, non-metastatic ES tumor tissues were sorted following one 3-week round of the 12 μ M treatment regimen. Sorted cells were then used to create new engineered bone tumors that were exposed to another round of 12 μ M linsitinib treatment regimen. Luminescence as a function of cancer cell number and viability was measured (mean \pm s.e.m., n=3, day 21, biologically independent per group). *P<0.05 by unpaired, two-tailed Student's t-test.

A

Negative Control

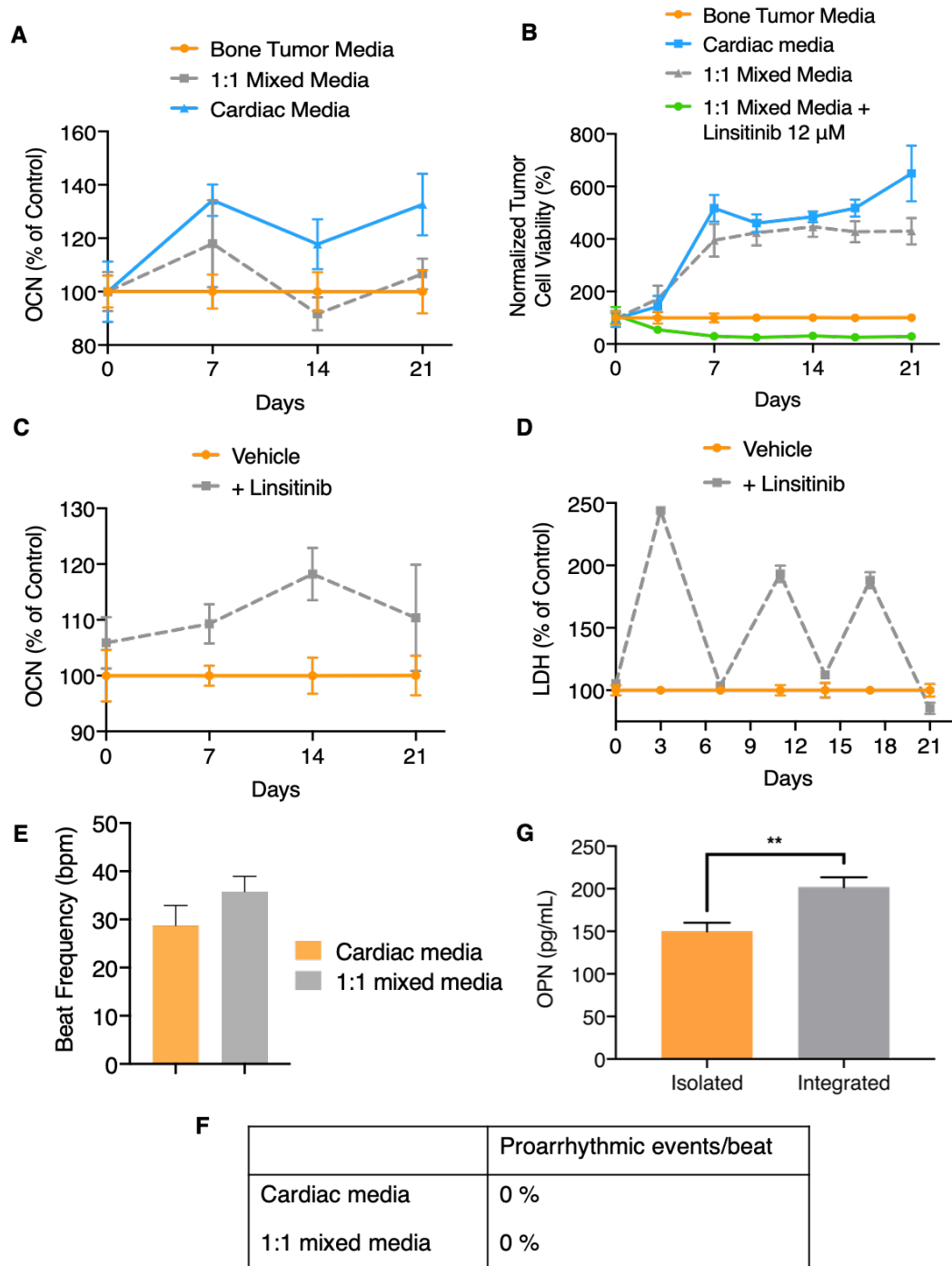


Linsitinib

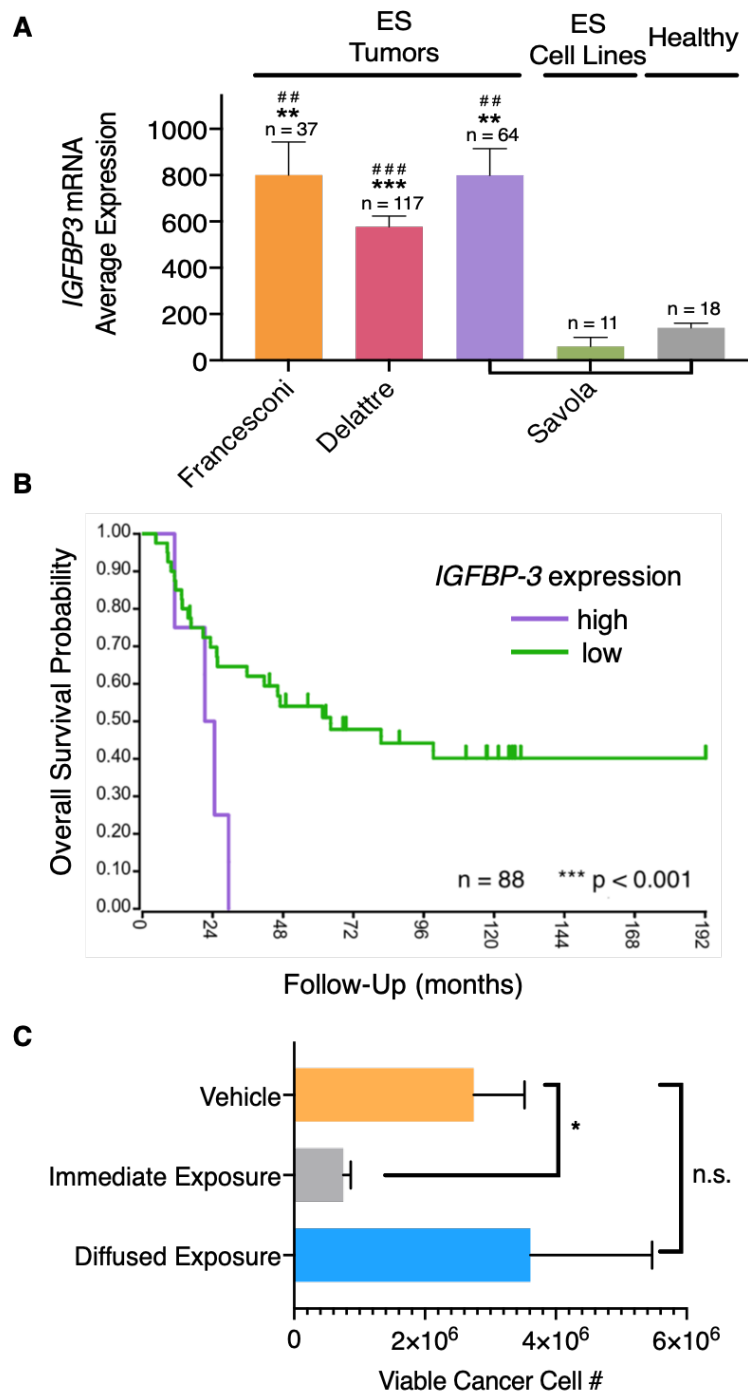
**B**

■ Negative Control
■ Linsitinib

Supplemental Figure 9. Calcium handling of cardiac tissues exposed to linsitinib in isolation. A. Representative traces of calcium transients. **B.** Calcium transients of cardiac tissues characterized by interbeat variability, time to peak and decay time (mean \pm s.e.m., n = 17-18). *P < 0.05 by unpaired two-tailed Student's t test.



Supplemental Figure 10. Assessment of the effects of integrated platform culture media conditions on engineered bone tumor and cardiac tissues. A. & B. Engineered non-metastatic ES bone tumors were grown in bone tumor media (isolated culture conditions), 1:1 mixed media (integrated platform conditions), or cardiac tissue media for 21 days. Supernatants collected every 7 days were then analyzed for secretion of OCN (osteoblast marker) (mean \pm s.e.m., n = 3). Samples were also analyzed every 3 days for luminescence values as a function of viable cancer cell number. **B., C. & D.** Engineered non-metastatic ES bone tumors grown under the integrated platform conditions (1:1 mixed media) were treated with linsitinib (12 μ M) according to the previously outlined 21-day clinical treatment regimen. Luminescence (B), OCN (C), and LDH secretion (D) as functions of cancer cell number and viability as well as osteoblast function and cytotoxicity, respectively, were measured (mean \pm s.e.m., n=3). **E.** Heart tissues were grown in either standard conditions (cardiac media) or under the integrated platform conditions (1:1 mixed media) and their beat frequency measured across 72 hours (mean \pm s.e.m., n=4). **F.** Occurrence of proarrhythmic events after the heart tissues being cultured under cardiac media or 1:1 mixed media (mean \pm s.e.m., n=4). **G.** Secretion of osteopontin (OPN) by bone tumor tissue grown for 3 days either in isolated culture or exposed to perfusion within the integrated platform (mean \pm s.e.m., n=4). Concentrations have been normalized to account for differences in volume between the two culture settings. *P < 0.05; **P < 0.01 by two-way ANOVA with Bonferroni post-test or unpaired two-tailed Student's t test.

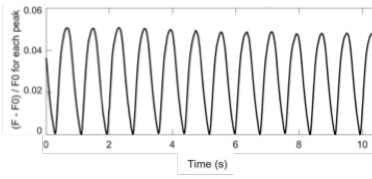


Supplemental Figure 11. Evaluation of IGFBP-3 expression and effects on survivability across ES patient populations and the role of drug diffusion in the response of non-metastatic engineered ES bone tumor to linsitinib in the integrated platform.

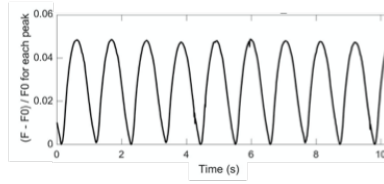
A. Genomic analysis of previously published, open access ES patient tumor, ES cell lines (2D culture), and healthy patient gene expression microarray data sets, specifically looking at average *IGFBP-3* mRNA expression (mean \pm s.d., n as indicated) Symbols: * for ES tumors vs ES cell lines grown in 2D culture, # for ES tumors vs healthy tissues. *, # P < 0.05; **, ## P < 0.01; ***, ### P < 0.001; by one-way ANOVA with Bonferroni post-test. **B.** Kaplan-Meier survival probability analysis performed looking at *IGFBP-3* gene expression in the Savola et al. ES patient data set and the overall survival probability, linked to it, across time (months) (n as indicated). A log-rank test that gave the lowest P-value was calculated to separate tumor samples expressing high and low *IGFBP-3* mRNA levels. **C.** Engineered non-metastatic ES bone tumors and cardiac tissues were exposed to linsitinib (12 μ M) over a period of 72 hours in the perfused integrated platform. Linsitinib was either introduced into the reservoir and allowed to circulate and diffuse into the tissues under physiologically relevant fluid flow conditions (diffused exposure) or it introduced directly into the tissue chambers (immediate exposure). Luminescence as a function of cancer cell number and viability was measured (mean \pm s.e.m., n = 4). *P < 0.05; **P < 0.01; ***P < 0.001; ****P < 0.0001 by unpaired two-tailed Student's t test.

A

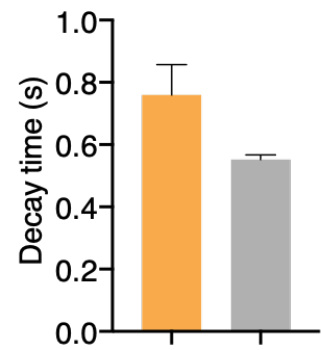
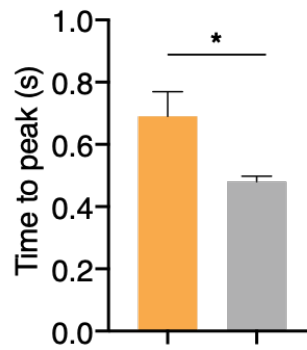
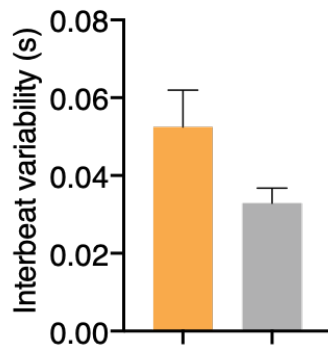
Negative Control



Linsitinib



B



■ Negative Control
■ Linsitinib

Supplemental Figure 12. Calcium handling of cardiac tissues exposed to linsitinib cultured in the integrated platform. A. Representative traces of calcium transients. **B.** Calcium transients of cardiac tissues characterized by interbeat variability, time to peak and decay time (mean±s.e.m., n =8-9). * $P < 0.05$ by unpaired two-tailed Student's t test.